GENERAL METHODOLOGY BASED ON DIMENSIONLESS PARAMETERIZATION FOR LIDAR PERFORMANCE ASSESSMENT

Ravil Agishev [(1)], Barry Gross [(2)], Adolfo Comeron [(3)], Fred Moshary [(2)], Samir Ahmed [(2)], Alexander Gilerson [(2)]

[(1)] Kazan State Technical University, 10, K.Marx St., Kazan, Tatarstan 420111, Russia, E-mail: ravil_agishev@mail.ru
[(2)] NOAA-CREST, City College of the City University of New York, 140 St. & Convent Ave., New York, NY 10031, USA, E-mail: gross@ccny.cuny.edu
[(3)] Polytechnic University of Catalonia, 1-3, Jordi Girona, Barcelona 08034, Spain, E-mail: comeron@tcs.upc.edu

ABSTRACT

In lidar development, maintenance and upgrading, the problem is posed of how to compare and estimate potential performance of existing and newly developed lidars with sometimes very different design approaches. Lidar designs vary widely depending on the specific application, technical specifications and requirements to be met, the hardware components available, financial limitations, developers experience and preferences, etc.

While simple qualitative design issues such as the use of a more powerful laser transmitter, a larger aperture receiving telescope, and/or more sensitive photoreceivers will obviously achieve a greater operation range, better retrieval accuracy etc., cost constraints often limit such designs. To conduct quantitative tradeoff studies, a significant number of instrumental parameters and external environmental factors must be taken into account, and it is often not clear from this representation how each subsystem and/or environmental parameter can quantitatively affect the ultimate performance.

Analysis of lidar performance is traditionally based on examination of the signal-to-noise ratio (SNR) at the photodetector output. While the comprehensive nature of the SNR criterion makes it a very useful tool for assessing a given lidar system, it is also a weak point, because it obscures the impact of the different components, which is desirable to be known by a system developer or user. For example, an increase or reduction of SNR can be caused not only by the scattering efficiency of the target under study, but also by changes in "weather" conditions for signal propagation, by changes of background conditions, or by other factors. If the influence of the different factors cannot be evaluated individually, it is difficult to evaluate subsystem or overall system measurement capabilities.

Following these considerations, we performed a series of works [1-4] to introduce a dimensionless parameterization methodology and to describe and assess the lidar system performance from different points of view. In the present work, we combine and bring together our recent results as a unified generalized methodology. It includes the dimensionless parameterization as a core component, and can be widely used to evaluate a broad range of lidar system capabilities for a variety of lidar remote sensing applications, as well as to serve a basis for selection of appropriate lidar system parameters for a specific application.

The main advantage of the methodology under discussion is that it provides generalized, uniform and objective approach for the evaluation of a broad range of lidar types and systems (aerosol, Raman, DIAL), operating on different targets (backscatter or topographic) and can be used within the lidar community to compare different lidar instruments.

1. SPATIAL-ANGULAR FILTERING EFFICIENCY

Criterion of spatial-angular filtering efficiency

For common monostatic biaxial lidar, the farther the pulse scattering volume gets from the apparatus, the less is the distance between the volume image and the receiving optics focal plane. So along the sounding process both shape and area of the scattering volume image are changed, and the instantaneous signal field of view is considerably less than the field of view for background radiation. We introduce a figure of merit J as a spatial-angular filtering efficiency criterion

$$J = \Omega_s / \Omega_0$$

where Ω_S is the signal field of view and Ω_0 is the receiver field of view. Practically, the Ω_0 is the background radiation angular field Ω_b (Ω_0=Ω_b), when the background fills up all the angular field of the receiving optics.

Spatial-angular filtering efficiency of typical lidars

a) Round diaphragm

Though for scattering signals coming from far atmosphere slices the image size will be considerably less than $W(R_{min})$, one chooses the field diaphragm diameter according to R_{min} taking into account the spot shift span from the optical axis (Fig.1). However, this leads to a very large angular field for the background radiation, and to a value J<<1, that may impair the measurement accuracy. The spatial-angular efficiency of such optical system is as follows [1]:

$$J_1 = [(d_0 / R + \Theta_0)/(\frac{d_0/2 + L}{R_{\min}} + \Theta_0)^2]^2$$

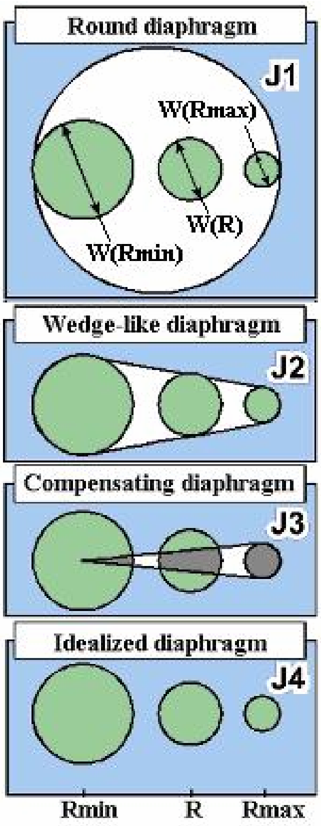

Fig.1. Cross-sections of signals gathered from ranges R_{min}, R, and R_{max}, for different field-stop diaphragms.

b) Wedge-like diaphragm

According to the form of the scattering-volume image trace, if the mutual orientation of the transmitter and receiver optics is fixed, a diaphragm shaped as the "image trace" would accept the lidar backscattered radiation from the R_{min} to R_{max} range [1] while limiting the background radiation reaching the detector. This trace looks like a wedge with round-shaped ends (Fig.1). Then the spatial-angular filtering efficiency of such a system (Fig.2) can be expressed as follows

$$J_2 = \frac{\pi}{2}\left(1+\frac{d_0}{R\Theta_0}\right)^2 / \left(2+\frac{d_0}{R_{mi}\Theta_0}\right)\frac{L}{R_{mi}\Theta_0} + \frac{\pi}{2}\left(1+\frac{d_0}{R_{mi}\Theta_0}\right)$$

c) R^2-factor compensating diaphragm

The non-round diaphragms of compensating type are intended for reducing the dynamic range of the received lidar signals (Fig.1). It can be shown that the following relations for the efficiency J_3 hold [1]:

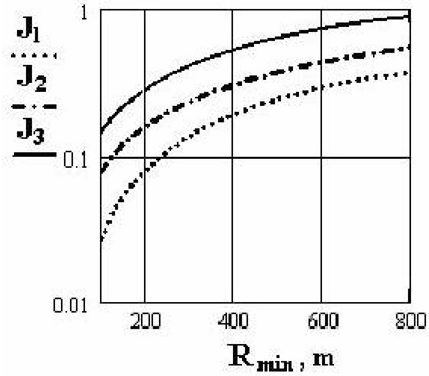

Fig.2. Spatial filtering efficiency J vs. R_{min} for optical systems with round (J1), wedge-like (2) and compensating (3) diaphragms at $\theta_0=10^{-3}$rad, f=1m, d_0=0.02m, L=0.5m.

$$J_3 = \frac{8\,[1 - x(R)/a_\infty]\Theta_0}{\pi\,\Theta_0 + 4a_\infty}$$

Thus, we conclude that common systems may have a very low spatial-angular filtering efficiency J against background radiation and it can be well less than 1. The spatial-angular-background filtering efficiency is very sensitive to the absolute value of R_{min} and can drop below of the 0.1 level, as shown in fig.2. Low values of the J figure of merit lead to very low signal/background ratio at the photodetector input which may result in poor measurement accuracy.

2. PREDICTION OF LIDAR PHOTODETECTOR PERFORMANCE IN PRESENCE OF SKY BACKGROUND

We developed a simple approach to predict APD/PMT lidar detector performance in presence the residual skylight background [4]. By introducing dimensionless signals and noises, we unified previously used approaches to an analysis of the influence of sky background noise on SNR and threshold sensitivity of a given generalized lidar receiver. We also introduced a system parameter U and developed simple expressions with dimensionless variables depending solely on the various signal and noise parameters to quantify the detector threshold degradation as well as the reduction in operating range under variable sky background conditions [3,4].

$$U \equiv P_t / P_{t0} = \frac{\Psi_s^{\min}}{\Psi_s^{\min}(\Psi_b = 0)} = \frac{1 + \sqrt{1 + \frac{4}{\rho^2}\Psi_n^2\left(1 + \frac{\Psi_b}{\Psi_n^2}\right)}}{1 + \sqrt{1 + \frac{4}{\rho^2}\Psi_n^2}}$$

where the normalized parameters of signal, background and internal noise were defined as follows: $\Psi_s \equiv P_s / P_q$, $\Psi_b \equiv P_b / P_q$, $\Psi_n \equiv P_n / P_q$, and P_s, P_b and P_q are the powers of a lidar echo-signal and background radiation at and the detector's quantum noise power, respectively.

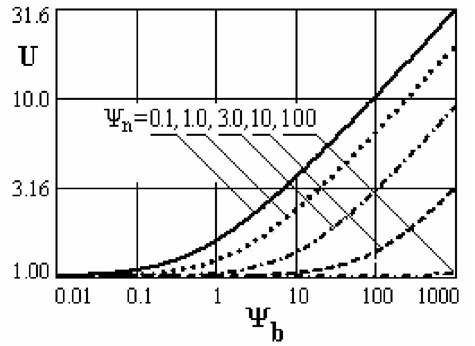

Fig.3. Lidar photodetector threshold sensitivity degradation due to external background.

It was shown, that for any lidar receiver, the inverted numerical value of the U-parameter defines a square of a normalized operation range of lidar r_B when accounting only the geometrical extinction of the echo-signal:

$$r_B \equiv \frac{R_B}{R_0} = \sqrt{\left[\sqrt{1+\frac{4}{\rho^2}\Psi_n^2\left(1+\frac{\Psi_b}{\Psi_n^2}\right)}-1\right]\Big/\left(1+\frac{\Psi_b}{\Psi_n^2}\right)\left(\sqrt{1+\frac{4}{\rho^2}\Psi_n^2}-1\right)} = U^{-1/2}$$

This allows lidarists to quickly predict the reduction of the lidar operation range on the basis of Ψ_b,Ψ_n alone as illustrated in Fig. 4. Of course, other atmospheric affects would complicate the analysis of relations between r_b and U.

In addition, by introducing a "generalized" spectral efficiency model for both PMTs and APDs which is built from an envelope of individual component responses, we performed a unified comparative analysis of the capabilities of typical lidar photodetectors for selected spectral regions under a wide variety of possible background noise levels. These generalized results can assist lidar researchers in selecting a photodetector most appropriate for given measurements.

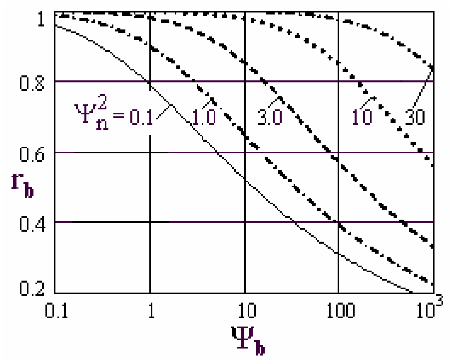

Fig. 4. Reduction of the lidar operating range due to the sky background for photodetectors with different internal noise levels (ρ=1).

These results allow the user to assess and predict the lidar photodetector behavior and make the reasonable choice of the best photodetector under different background conditions.

3. PARAMETERIZATION METHODOLOGY FOR LIDAR SYSTEM ASSESSMENT

The signal to noise ratio at the lidar photodetector output can be decomposed as a product of five independent dimensionless parameters, each of which follows from a different source [2].

$$\Psi_X = V\, Q_X\, W^2\, U^{-1}\, r^{-2}, \tag{1}$$

The V-parameter is defined as the ratio of the echo-signal power P_{s0} received from the reference range R_0 for the reference molecular atmosphere to the photodetector threshold power P_{t0} in the absence of background noise [2,3]: $V = P_{s0}/P_{t0}$.

The Q_X-parameter in Eq. (7) simply describes the backscatter efficiency of an arbitrary species to the molecular reference. In particular, for aerosol backscattering lidar:

$$Q_{BS}(\lambda,\lambda_0) = \frac{\beta_a(\lambda)+\beta_m(\lambda)}{\beta_m(\lambda_0)}$$

Table. Range of Q_X-parameter

Lidar type	Topogr. lidar	Elastic lidar		Raman lidar	
		Aerosol atmosphere	Molecular atmosphere	N_2	H_20
Q_x	$10^2\ldots10^4$	$10^0\ldots10^2$	$10^{-1}\ldots10^1$	$10^{-5}\ldots10^{-3}$	$10^{-7}\ldots10^{-5}$

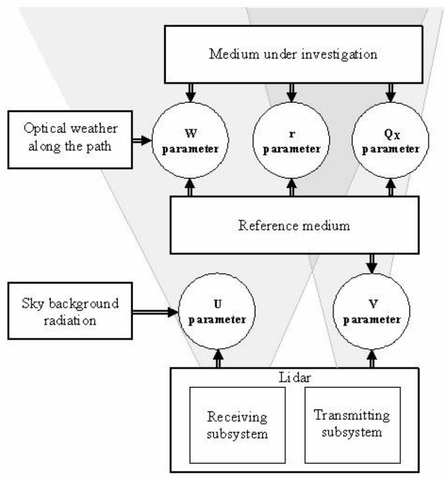

Fig. 5. Interrelations between dimensionless lidar parameters introduced.

The schematics in Fig. 5 shows the relationships between the normalized parameters and the components of the measuring system including the atmospheric state, the lidar transmitter/receiver, background noise and the reference medium, is traced.

The third factor in Eq. (1) is a normalized atmospheric component W that is determined by transparency ratio of the atmosphere state and the standard molecular atmosphere:

$$W_{BS} = \frac{T(\lambda_L, R)}{T_0(\lambda_L, R_0)} = \exp\{-\int_0^R [\alpha_a(R', \lambda_L) + \alpha_m(R', \lambda_L)] R' \, dR' - \alpha_0(\lambda_L) R_0\}$$

U-parameter characterizes the influence of the background clutter to the lidar threshold power of the according to expressions. The r-parameter is a normalized range-factor that allows comparing the current range R with the initial range R_0.

On the basis of the dimensionless parameterization a number of important predictions can be performed.

For example, a prediction of maximum operation range of lidar vs. Q_X-parameter under different optical weather conditions (a molecular atmosphere, light and dense haze and a fog in absence of background clutter are shown in Fig.6.

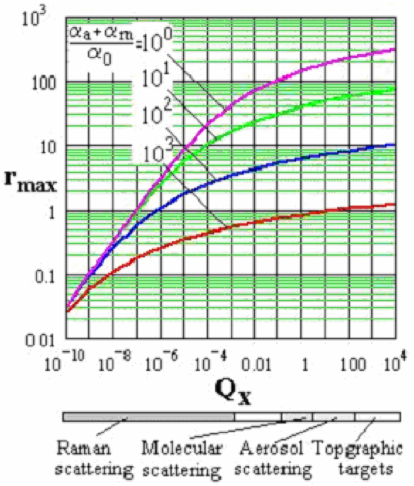

Fig. 6. Maximum operation range vs. Q_X-parameter under different optical weather conditions at λ=550 nm for $V=10^7$ in absence of background clutter. R_0=1 km.

This allows the user to estimate maximum operation range of any lidar by use only a few dimensionless parameters introduced.

Estimations of lidar performance for different energy potential V and backscatter efficiencies Q_x under different sky background conditions are shown in Fig.7. They give general idea about the potentially achievable operation range under real sky background conditions.

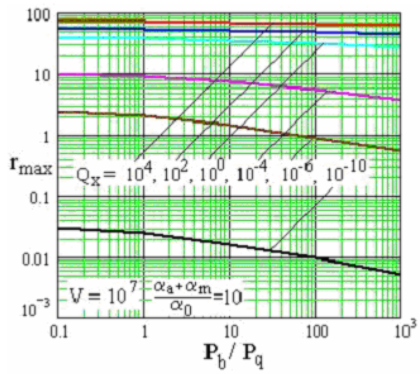

Fig. 7. Lidar operation range vs. normalized background power for different Q_X- and V-parameters. Optical weather: $(\alpha_a+\alpha_m)/\alpha_0$ =10. R_0=1 km.

4. CONCLUSIONS

In this paper, a general method for the validation and performance comparison of various lidar systems is discussed. The method is based on a decomposition of the total SNR into five dimensionless parameters representing the transmitter and receiver conditions, background noise, target efficiency, atmospheric operation conditions and a scale length.

The main advantage of this approach is that it provides generalized, uniform and objective criteria for the evaluation of a broad range of lidar types and systems (aerosol, Raman, DIAL), operating on different targets (backscatter or topographic) and can be used within the Lidar community to compare different lidars.

Acknowledgements. The authors acknowledge partial support of this work by grants from NOAA # NA17AE1625 and NASA # NCC-1-03009.

5. REFERENCES

1. Agishev R. and Comeron A. Spatial filtering efficiency of biaxial monostatic lidar: Analysis and applications, *Applied Optics*, vol. 41, No.36, 7516-7521, 2002.
2. Agishev R., Comeron A., Gross B., Moshary F., Ahmed S., Gilerson A. Application of the method of decomposition of lidar signal-to-noise ratio to the assessment of laser instruments for gaseous pollution detection, *Applied Physics B*, vol. 79, No.2, 255-264, 2004.
3. Agishev R., Gross B., Moshary F., Ahmed S., Gilerson A., Development of a SNR parameterization scheme for general lidar assessment, *Applied Physics B*, vol. 80, No. 6, 765-776, 2005.
4. Agishev R., Gross B., Moshary F., Gilerson A., Ahmed S., Simple approach to predict APD/PMT lidar detector performance under sky background using dimensionless parameterization / *Optics and Lasers in Engineering*, vol. 44 (2006, in press).